https://doi.org/10.5194/egusphere-2026-1128
Preprint. Discussion started: 6 March 2026


# Unified Patterns of Topological Structure of Hydrological Characteristics in Global River Networks

Chensong Zhao[1], Qihua Ke[1], Yuan Cao[1], Shutong Liu[1], Randongfang Wei[1], Di Xie[1], Jinqiang Wang[1], Jingwei Huang[1], Qingqing Zhang[2], Jiahui Gao[2], Jing Li[2], Guangqian Wang[1,2], Deyu Zhong[1,2]

[1]State Key Laboratory of Hydroscience and Engineering, Tsinghua University, Beijing, 100084, China
[2]Joint-Sponsored State Key Laboratory of Plateau Ecology and Agriculture, School of Water Resources and Electric Power, Qinghai University, Xining, 810016, China

*Correspondence to*: Deyu Zhong (zhongdy@tsinghu.edu.cn)

**Abstract.** Unravelling the coupling between river network structure and hydrological fluxes is essential for understanding basin-scale dynamics. While traditional ordering methods describe macro-scale patterns, they often obscure local functional variations. This study quantifies the universal hydrological patterns of global river networks by integrating the classical Horton–Strahler framework with a hierarchical pyramid decomposition technique. Leveraging the global HydroATLAS dataset, we analysed 228 representative basins spanning diverse hydro-climatic regimes. We extracted rigorously defined network attributes and hydrological fluxes to examine the scaling behaviours of fundamental structural components, defined here as basic units. Our results reveal a striking topological invariance in hydrological characteristics across both varying spatial scales and distinct geographic regions. Specifically, the runoff and discharge ratios of these basic units maintain robust statistical consistency regardless of basin size or climatic conditions ranging from humid to arid. This suggests that network topology functions as a dominant physical control, effectively acting as a low-pass filter that dampens high-frequency climatic variability to produce unified global scaling laws. These findings advance the theoretical understanding of fractal river networks. Furthermore, they open new avenues for prospective research, including the integration of these physics-informed topological priors into next-generation Earth system models to improve discharge predictions and water resource modelling in ungauged basins.

## 1 Introduction

Rivers constitute the fundamental vascular system of continental landscapes, functioning simultaneously as conduits for water and sediment transport and as critical corridors for ecological and biogeochemical fluxes (Leopold et al., 1964). Understanding river structure is fundamental for explaining how these systems function and interact with surrounding landscapes (Ward et al., 2002; Thorp et al., 2006; Gurnell et al., 2016). Recent geomorphological inquiry demonstrates that river network evolution is governed by deterministic self-organization principles rather than stochastic randomness, emerging from the complex interplay between climatic forcing and tectonic constraints (Whittaker, 2012; Perron et al., 2012; Li et al., 2023; Sassolas-Serrayet et al., 2018). This inherent complexity gives rise to distinctly different regional patterns, necessitating differentiated

https://doi.org/10.5194/egusphere-2026-1128
Preprint. Discussion started: 6 March 2026


methodological approaches when analysing river network structures across varied geographical regions (Schmitt et al., 2018; Jaeger et al., 2014; Güneralp et al., 2012).

Consequently, topological frameworks have become instrumental in deciphering river network architecture, aiming to identify universal scaling laws and invariant properties that persist throughout landscape evolution. Horton (1945) pioneered this quantitative approach by introducing a hierarchical ordering system, which established the foundational scaling laws governing stream numbers, lengths, and drainage areas. Subsequently, Strahler (1957) refined this framework, developing the Horton–Strahler (H–S) ordering method which has proven widely applicable to both riverine and biological vascular networks (Dodds and Rothman, 2000b). As an alternative perspective, the Shreve–Smart ordering method focuses on stream segments between confluences, offering complementary insights into network topology (Smart, 1972; Shreve, 1966). These methodological frameworks collectively have facilitated a coherent understanding of river network organization, revealing self-similar structures that demonstrate remarkable consistency across diverse spatial and temporal scales (Zanardo et al., 2013; Rodriguez-Iturbe and Rinaldo, 1997).

Early topological investigations were fundamentally constrained by the scarcity of high-resolution digital elevation models (DEMs), which limited both the accuracy of network extraction and the geographic scope of analysis. However, contemporary advances in remote sensing technology and geographic information systems (Lindsay and Dhun, 2015; O'callaghan and Mark, 1984; Li et al., 2004; Farr et al., 2007), coupled with enhanced computational capabilities and improved extraction algorithms (Demarchi et al., 2017; Sangireddy et al., 2016b; Pelletier, 2013; Ortega and Rueda, 2010; Hou et al., 2011; Gong and Xie, 2009; Bai et al., 2015b), now enable comprehensive analyses of river network structures through geospatial approaches. These technological advancements have revolutionized the acquisition of hydro-geomorphic data, enabling the precise characterization of channel geometries and network topology at global scales (Gurnell et al., 2016; Linke et al., 2019; Bai et al., 2015a). For instance, one study has extracted river network data at a 30 m resolution using H–S and Shreve–Smart ordering methods to examine traditional Horton laws and the statistical characteristics of inner and outer chains within river network pyramid units (Bai, 2015), while another study employed width topological functions to enhance the physical interpretation of river networks (Heasley et al., 2019). Despite these methodological advances, analyses of structural patterns reveal an inherent equivalence among parameters describing river networks (Zhang et al., 2009; Mcconnell and Gupta, 2008; Dodds and Rothman, 2000a), indicating fundamental self-similarity (Peckham, 1995a; Peckham, 1995b; Peckham and Gupta, 1999; Veitzer and Gupta, 2000). Many river structure parameters, such as river quantity and length, rely on hierarchical descriptions that aggregate or average the topological and geometric properties of river networks, reflecting overall characteristics while failing to distinguish local variations (Tejedor et al., 2017; Czuba and Foufoula-Georgiou, 2015). Additionally, traditional structural parameters struggle to elucidate differences between various rivers, rendering them inadequate for differentiating distinct river structures (Różycka and Migoń, 2021). Therefore, there is a pressing need for high-resolution descriptive metrics capable of resolving local structural features and linking them explicitly to hydrological fluxes, thereby advancing the theoretical understanding of structure-function coupling in river basins (Thober et al., 2019).

https://doi.org/10.5194/egusphere-2026-1128
Preprint. Discussion started: 6 March 2026


Recent investigations into river network topology have made significant advances in understanding structural characteristics, though it has remained necessary to further integrate these findings with hydrological attributes influenced by network configurations. Rivers function as carriers of runoff and discharge variations, both of which should inherently align with the network's topological characteristics (Rinaldo et al., 2014). Expanding research to strengthen connections between structural analysis and hydrological elements offers promising pathways for enhancing our understanding of how river network topology influences hydrological processes – relationships that are instrumental for informed water resource management, improved flow prediction, and ecological conservation (Sangireddy et al., 2016a; Salazar et al., 2018; Lane et al., 2018; Bogale, 2021). Theoretically, these universal hydrological patterns emerge as a direct consequence of the optimal channel network (OCN) hypothesis (Rinaldo et al., 2014), which posits that river networks evolve to minimize total energy dissipation. If network topology is indeed governed by energy minimization principles (Banavar et al., 1999), it follows that the hydrological fluxes constrained by this topology should exhibit scale-invariant statistical consistency across diverse hydro-climatic regimes.

This research aims to address knowledge gaps by exploring hydrological characteristics across diverse topological structures in global river networks. Our primary objective is to quantify universal patterns and examine their invariance within hydrological contexts. The study leverages an extensive global dataset encompassing river networks and their associated hydrological parameters. Methodologically, we apply the H–S ordering framework to analyse modified traditional ordering features, while implementing river network pyramid decomposition techniques to isolate fundamental network units. This integrated approach facilitates comprehensive computation and statistical analysis of hydrological-topological characteristics across global river systems, thereby advancing our understanding of the intrinsic relationships between river network structure and hydrological function.

Finally, our research further explores the relationship between geometric parameters and hydrological-topological characteristics of global river networks. Through systematic comparison of these findings with inherent topological structures, we attempt to elucidate consistency patterns that emerge throughout the evolutionary processes of river networks. This integrated analysis will enhance the theoretical understanding of coupling relationships between river network structure and hydrological function. The results of this study will contribute to establishing a more robust framework for interpreting river network dynamics across different geological and climatic settings. In the context of increasing environmental variability, this work provides practical and valuable insights for watershed management and hydrological modelling.

## 2 Data and methods

In this study, we utilize river network data from HydroATLAS, along with corresponding hydrological elements. We first introduce runoff and discharge ratios for graded river networks based on the branch ratio from the traditional H–S ordering method. Then, we extract basic river network units through pyramid decomposition by incorporating the definitions of inner and outer links from the Shreve–Smart ordering method. Through this framework, we can define the concepts of runoff and

https://doi.org/10.5194/egusphere-2026-1128
Preprint. Discussion started: 6 March 2026


discharge ratios for river segments with various confluence configurations, for basic units of different characteristic lengths, and for the inner and outer chains within these basic units.

### 2.1 Data selection and variable identification from the HydroATLAS dataset

The HydroATLAS dataset is derived from the HydroSHEDS database, a project initiated by the World Wildlife Fund (WWF) in the United States (Lehner et al., 2008). This comprehensive resource reformats raw data from global digital maps to derive hydrological environmental attributes, linking them to multi-scale nested sub-basins and individual river segments extracted from the global HydroSHEDS database, with a resolution of 15 arc seconds (Linke et al., 2019). The dataset architecture consists of two complementary components: BasinATLAS and RiverATLAS. Notably, the inherent topological information in HydroATLAS supports essential network functions, such as identifying upstream and downstream connections, making it particularly valuable for river network analysis. It is important to note that the HydroATLAS network is topologically pre-processed to enforce a dendritic structure, effectively resolving bifurcations and reticulate loops into single flow paths (Lehner et al., 2008). Consequently, our analysis focuses on the robust topological backbone of river systems, excluding the secondary complexities of local reticulation.

The RiverATLAS dataset comprises approximately 8.5 million river segments and 56 hydrological environmental variables, categorized into 281 distinct attributes (Linke et al., 2019). This extensive dataset provides comprehensive coverage of global river systems while maintaining detailed attribute information for each segment. Given the substantial volume of data and the complexity of hydrological variables, a systematic approach to data filtering and attribute selection is necessary for effective analysis.

For our research purposes, we identified and selected key attributes from the RiverATLAS dataset in Table 1. These parameters include essential river network attributes such as segment identification (HYRIV_ID), downstream connectivity (NEXT_DOWN), basin outlet identification (MAIN_RIV), Horton–Strahler ordering classification (ORD_STRA), and catchment area (CATCH_SKM). Regarding hydrological variables, we specifically selected mean annual runoff depth (run_mm_cyr, abbreviated as RMC) and mean annual discharge (dis_m3_pyr, abbreviated as DMP). Notably, RMC represents runoff data over the entire catchment surface, while DMP quantifies discharge data at the basin outlet. The hydrological attributes in HydroATLAS are derived from the WaterGAP model (Döll et al., 2003), which has been extensively calibrated against thousands of discharge stations (GRDC) worldwide (Lehner and Grill, 2013). While local deviations may exist, this dataset provides a spatially consistent and mass-conserving framework essential for global-scale topological analysis, avoiding the spatial fragmentation often found in gauge-based observations.

To ensure the statistical robustness of the scaling analysis, strict screening criteria were applied to the global dataset. River basins were selected only if they contained complete HS orders ranging from 1 to 7. A minimum threshold of 1,000 river segments per network was established to guarantee sufficient sample sizes for the calculation of statistical moments at each order. Based on these criteria, 228 representative river basins were identified globally. These basins cover approximately 78 % of the global watershed area and span diverse hydro-climatic zones, including 14 basins in the Arctic and Greenland in

https://doi.org/10.5194/egusphere-2026-1128
Preprint. Discussion started: 6 March 2026


Table 2. This extensive coverage minimizes regional bias and ensures that the derived topological laws represent a truly global pattern.

Table 1. River network attributes and matching hydrological environment variables.

| Parameter Category | Parameter Name | Unit | Parameter Explanation |
|---|---|---|---|
| River network attribute data | HYRIV_ID | \ | Segment ID used to distinguish different river segments |
| | NEXT_DOWN | \ | Downstream segment ID of the river segment |
| | MAIN_RIV | \ | River segment ID at the basin outlet, used to identify the entire river network |
| | ORD_STRA | \ | River segment order determined by the H–S ordering method |
| | CATCH_SKM | $km^2$ | Catchment area of the river segment |
| Hydrological variable | run_mm_cyr (RMC) | mm | Mean annual runoff depth |
| | dis_m3_pyr (DMP) | $m^3\ s^{-1}$ | Mean annual discharge |

Table 2. Regional distribution of the 228 representative river basins.

| Region | Number of River Networks |
|---|---|
| Africa | 48 |
| Europe and Middle East | 36 |
| Siberia | 18 |
| Asia | 30 |
| Oceania | 24 |
| South America | 29 |
| North and Central America | 29 |
| Arctic Region | 10 |
| Greenland | 4 |
| Global Total | 228 |

### 2.2 Runoff and discharge ratios from the H–S ordering method perspective

The Horton–Strahler (H–S) ordering method (Strahler, 1952) provides a hierarchical classification of river segments within a network (Fig. 1a). According to these rules: (1) the smallest tributaries at the source are designated as first-order rivers; (2) when two rivers of the same order ω converge, the downstream river is classified as $\omega + 1$; (3) when rivers of different orders converge, the downstream river takes the higher order of the tributaries; and (4) the order $\Omega$ of the main river represents the highest order within the entire river network.

https://doi.org/10.5194/egusphere-2026-1128
Preprint. Discussion started: 6 March 2026


The river branch ratio $R_B(\omega)$, first proposed by Horton (1945), quantifies the relationship between the number of river segments of consecutive orders and is calculated following Eq. (1):

$$R_B(\omega) = \frac{N_{\omega-1}}{N_\omega}, \omega = 2,3,\ldots\Omega\ , \quad (1)$$

where $N_{\omega-1}$ and $N_\omega$ represent the number of river segments at order $\omega - 1$ and order $\omega$, respectively, and $\Omega$ indicates the highest order in the river network. Horton (1945) demonstrated that within a complete watershed, the number of rivers approximates a geometric series, suggesting that the river branch ratio $\tilde{R}_B$ remains approximately constant across different orders. Similar patterns and conclusions have been established for river length, watershed area, network density, and river slope (Schumm, 1956).

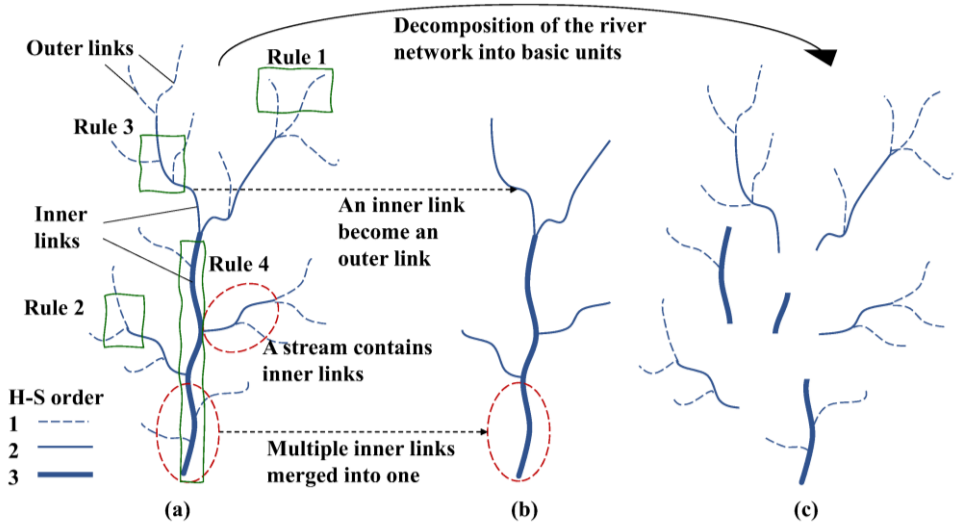


**Figure 1. Topological structure and component classification of river networks. (a) Original river network containing order 1 to 3 rivers. The section in the green boxed line shows the rules for H–S ordering method. (b) The new river network after the removal of the first-order rivers, which is also the mainstem basic units of the original network. (c) Basic units of tributaries obtained by decomposition of the original river network.**

To extend the concept of topological self-similarity to the hydrological domain, we define two analogous scaling metrics: the river runoff ratio $R_r(\omega)$ and the river discharge ratio $R_d(\omega)$. These ratios are calculated using Eq. (2) and Eq. (3), respectively:

$$R_r(\omega) = \frac{\sum r_\omega}{\sum r_{\omega-1}}, \omega = 2,3,\ldots\Omega\ , \quad (2)$$

$$R_d(\omega) = \frac{\bar{d}_\omega}{\bar{d}_{\omega-1}}, \omega = 2,3,\ldots\Omega\ , \quad (3)$$

where $\sum r_\omega$ and $\sum r_{\omega-1}$ represent the cumulative runoff for order $\omega$ and order $\omega - 1$ rivers, while $\bar{d}_\omega$ and $\bar{d}_{\omega-1}$ denote the mean river discharge for the same orders. The cumulative runoff for each river segment is derived by multiplying the RMC

https://doi.org/10.5194/egusphere-2026-1128
Preprint. Discussion started: 6 March 2026


and CATCH_SKM variables, expressed in cubic metres ($m^3$). The river discharge values are obtained directly from DMP data. Since runoff represents data across the entire watershed area, cumulative values are appropriate for calculating totals. In contrast, discharge reflects the flow at specific watershed outlets, making mean values more suitable for comparative analysis. When accumulating runoff data, $\sum r_\omega$ can be directly calculated by summing the runoff values of all river segments at the same order $r_\omega$. However, for the calculation of $\bar{d}_\omega$, only the discharge from the most downstream river segment is included for adjacent segments at the same H–S order. This ensures that connected segments are treated as a single integral river unit, thereby avoiding the bias of averaging multiple upstream segments.

We explicitly test the hypothesis that cumulative runoff and discharge adhere to a geometric progression across stream orders, analogous to Horton's laws of stream numbers and lengths. Taking the runoff ratio as an example, we specifically examine whether $R_r(\omega)$ can be approximated as a constant $\tilde{R}_r$ following Eq. (4):

$$\sum r_\omega = \sum r_1 (\tilde{R}_r)^{\omega-1}, \omega = 2,3, \dots \Omega \,, \tag{4}$$

Taking the natural logarithm of both sides yields Eq. (5):

$$ln(\sum r_\omega) = ln(\tilde{R}_r) \times \omega + b, \omega = 2,3, \dots \Omega \,, \tag{5}$$

In this equation, $\omega$ represents the independent variable, and $\sum r_\omega$ is the dependent variable. Through logarithmic linear regression, we obtain the slope $k$, from which $e^k$ can be computed to derive $\tilde{R}_r$, the characteristic runoff ratio of the river network.

### 2.3 Basic units of river network structure

The Shreve–Smart (S–S) ordering method (Smart, 1967; Shreve, 1966) enhances the H‑S framework by introducing the concepts of inner and outer links (Fig. 1a). The H–S order of outer links is defined as 1, while the H–S order of inner links is determined by the H–S orders of the upstream confluence segments. When consecutive river segments with identical H–S order connect from upstream to downstream, they are classified as inner link rivers. River segments can be categorized into outer link segments and inner link segments based on their properties, with rivers typically consisting solely of inner link rivers. Building upon the improved H–S ordering method derived from the S–S framework, researchers employ a hierarchical pyramid approach to extract river networks (Bai et al., 2015b). This hierarchical pyramid approach systematically decomposes the river network into its constituent “basic units”, thereby elucidating the fundamental aggregation processes that construct the complex topology of natural river systems (Fig. 1b and Fig. 1c). This method serves as a method for the stratification of the drainage network, where the order of the drainage network is defined by the minimum H–S order among all river segments. The original drainage network, extracted from the digital elevation model (DEM), possesses an order of 1, determined by its minimum H–S order for outer links.

Through iterative application of the hierarchical pyramid method, it is possible to generate a series of drainage networks at progressively higher orders. For example, an $n+1$ order drainage network can be derived from an $n$ order network, continuing

https://doi.org/10.5194/egusphere-2026-1128
Preprint. Discussion started: 6 March 2026


until the highest possible order $\Omega$ is achieved. The original order 1 drainage network (Fig. 2a) generates a new order 2 network (Fig. 2b), which subsequently yields an order 3 network (Fig. 2c) composed solely of outer links. In this context, segments with an H–S order equal to $n$ are designated as outer links, whereas those with an H–S order greater than $n$ are classified as inner links. Crucially, the derivation of higher-order sub-networks requires the strict conservation of mass and area; the hydrological attributes of pruned outer links must be integrated into the adjacent inner links to preserve the system's total budget (Dodds and Rothman, 2000c). Instead, the sub-watersheds and terrain attributes of these outer links must be systematically merged into the sub-watersheds or inner links to which they connect (Bai et al., 2015b), thereby preserving essential hydrological and geomorphological information throughout the hierarchical transformation process. Specifically, the pruning algorithm enforces strict mass conservation by aggregating the catchment area and cumulative runoff of each removed outer link into the nearest downstream inner link node. This ensures that the total hydrological fluxes at the basin outlet remain invariant across all hierarchical levels of the pyramid decomposition.

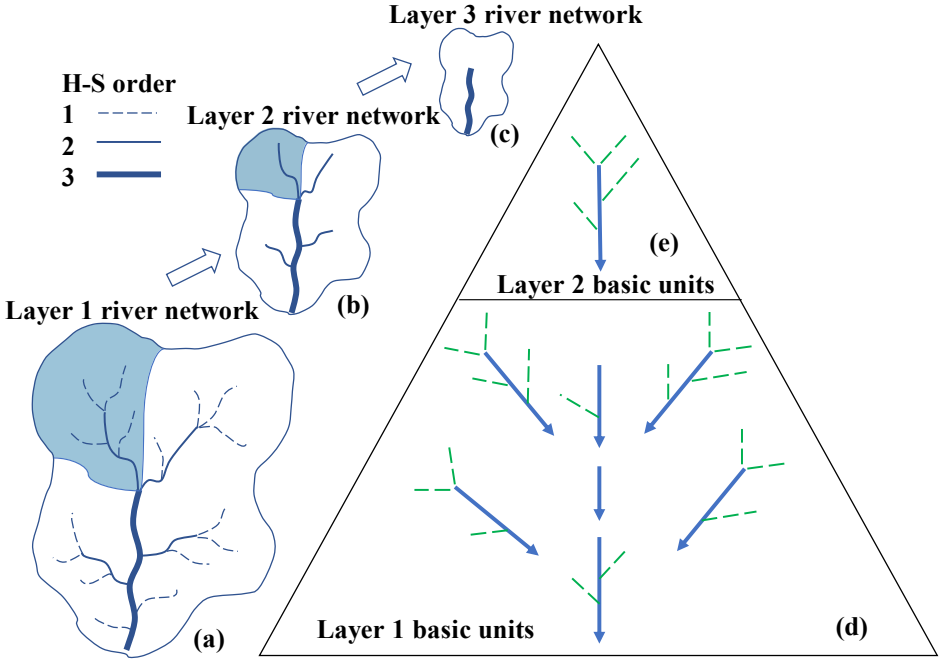


**Figure 2. Hierarchical decomposition of river networks using the pyramid approach. (a) Original river network with complete tributary structure. (b) Second level of the river network pyramid after systematic removal of first-order rivers. The attributes from blue regions in (a) have been consolidated and integrated together. (c) Third level of the river network pyramid following removal of second-order rivers. (d) Basic structural units extracted during the formation of the second pyramid level, representing the fundamental building blocks of network organization at this scale. (e) Basic units generated during the formation of the third level of the river network pyramid.**

As the pyramid structure develops, inner rivers and their adjacent pruned outer links converge to form the basic units of the river network (Fig. 2d and Fig. 2e). These units possess distinct inner and outer attributes and characteristic lengths. A basic

https://doi.org/10.5194/egusphere-2026-1128
Preprint. Discussion started: 6 March 2026


unit formed by two upstream outer links is defined as an outer unit; all other configurations are classified as inner units. The characteristic length of a basic unit is defined by the number of inner links that comprise it, providing a measure of structural complexity. Geometric length is highly sensitive to local geomorphic factors such as sinuosity and DEM resolution. In contrast, topological length serves as an intrinsic metric of the branching process, effectively filtering out high-frequency geomorphic noise to reveal the underlying network skeleton. This extraction approach not only reveals the hierarchical organization of drainage networks but also reduces dependence on data resolution. It has a significant advantage over methods that designate only the lowest-order segments as outer links, which are highly sensitive to DEM resolution (Fekete et al., 2001; Yang et al., 2014; Zhang and Montgomery, 1994). This "basic units" extraction approach conceptually aligns with the side-branching statistics described in the Tokunaga taxonomy (Tokunaga, 1978). By isolating these fundamental structural components, we can explicitly examine whether the hydrological self-similarity persists at the sub-network scale, independent of the overall basin magnitude (Zanardo et al., 2013).

The interplay between basic units and the river network pyramid is particularly noteworthy (Fig. 3): starting from a primary $\Omega$ order trunk stream, the emergence of the finest first-order tributaries occurs after $\Omega - 1$ expansions. During each expansion phase, river segments extend based on specific basic units, with these units varying in length and exhibiting diverse confluence patterns, even among segments of identical length. Consequently, a single trunk stream can theoretically evolve into an infinite array of structural configurations. By incorporating specific basic unit types during expansion, the trunk stream can develop characteristics that mirror any actual river system on Earth. The integration of the S–S ordering method with the hierarchical pyramid approach thus provides a comprehensive framework for analysing and understanding the complex structural patterns that define river networks across diverse geographical settings (Bai et al., 2015b).

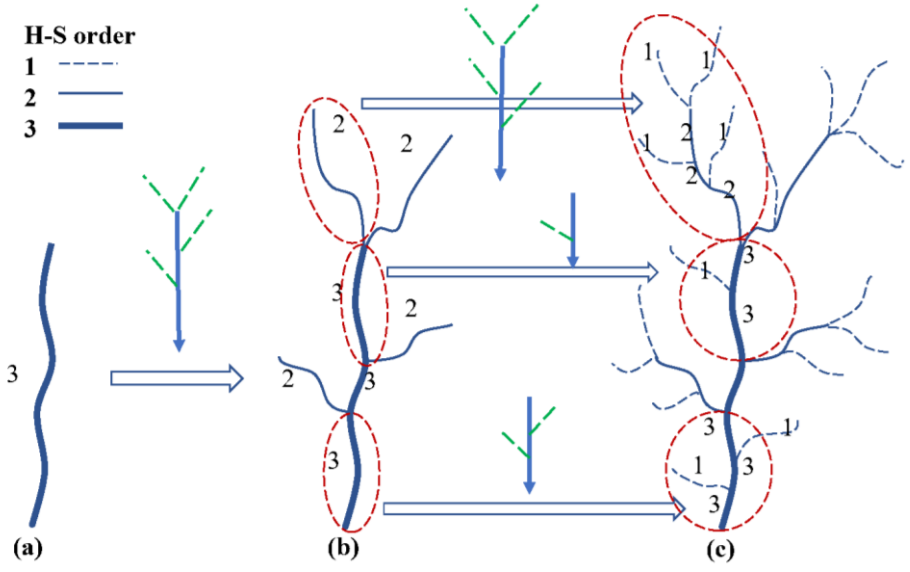


**Figure 3. Hierarchical topological structure of the river network. (a) Main stream of rivers with the highest order 3. (b) Order 2 tributaries emerge after a single expansion. (c) Eventually extension to the emergence of order 1 source tributaries.**

https://doi.org/10.5194/egusphere-2026-1128
Preprint. Discussion started: 6 March 2026


### 2.4 Parameters characterizing the hydrological topology of the basic unit

Based on the inner and outer attributes of the basic units, as well as their characteristic lengths, we can define the average cumulative runoff $R(\lambda)$ and the average discharge $D(\lambda)$ for basic units of different characteristic lengths. The calculation method for runoff and discharge within each basic unit follows a similar approach to $\sum r_\omega$ and $\bar{d}_\omega$ calculations. For multiple basic units sharing the same characteristic length, we compute the mean values to derive $R(\lambda)$ and $D(\lambda)$. This averaging approach is methodologically justified by the nested relationships and scale differences existing between basic units, providing a more rational quantification. Furthermore, by introducing the concepts of inner and outer units, we can define the average cumulative runoff ($R^{in}(\lambda)$ or $R^{out}(\lambda)$) and the average discharge ($D^{in}(\lambda)$ or $D^{out}(\lambda)$) for basic units of different characteristic lengths within these categories.

Similar to the H – S ordering method, the runoff ratio and discharge ratio of the inner and outer links of the basic units are defined as following Eq. (6) and Eq. (7):

$$R_r^{unit} = \frac{\sum r^{out}}{\sum r^{in}}, \tag{6}$$

$$R_d^{unit} = \frac{\sum d^{out}}{\sum d^{in}}, \tag{7}$$

where $\sum r^{out}$ and $\sum r^{in}$ denote the cumulative runoff for the inner and outer links of the basic units, while $\sum d^{out}$ and $\sum d^{in}$ refer to the cumulative discharge for these links. The calculation methods for these sums align with those for $\sum r_\omega$ and $\overline{d_\omega}$. Furthermore, by introducing the concepts of inner and outer units, we can define the runoff ratio ($R_r^{unit\_in}$ or $R_r^{unit\_out}$) and the discharge ratio ($R_d^{unit\_in}$ or $R_d^{unit\_out}$) within different categories.

This comprehensive framework enables a detailed analysis of the hydrological characteristics of the river network's basic units, reflecting the local attributes and characteristic patterns represented by basic units as rivers expand layer by layer.

## 3 Result

### 3.1 Statistical patterns of runoff ratios and discharge ratios from the H–S ordering perspective

To observe the statistical patterns of cumulative runoff and mean discharge across different river grades globally, we normalized the runoff and discharge data for representative rivers and created box plots (Fig. 4). As anticipated, first-order streams collectively account for the highest magnitude of cumulative runoff. This magnitude decays progressively with increasing stream order, closely approximating an exponential distribution characteristic of fractal networks. Conversely, seventh-order rivers show the highest mean discharge, which increases with river grade, also following an exponential distribution trend. These characteristics validate the feasibility of estimating $\tilde{R}_r$ and $\tilde{R}_d$ using logarithmic fitting methods.

https://doi.org/10.5194/egusphere-2026-1128
Preprint. Discussion started: 6 March 2026


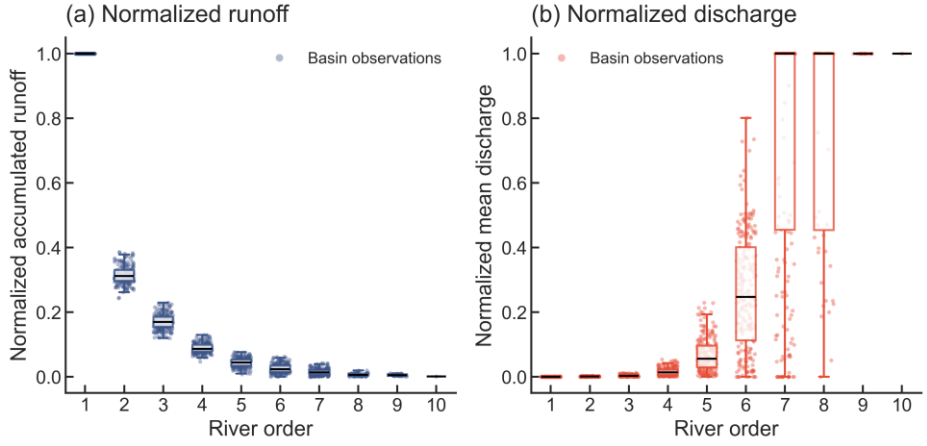


**Figure 4. Global statistics of normalized hydrological fluxes across hierarchical orders. (a) Normalized box plots of cumulative runoff from globally representative catchments. (b) Normalized box plots of mean discharge in representative global catchments. Data are normalized by the basin-maximum values to enable cross-scale comparison.**

Using two methods, we calculated the runoff and discharge ratios for 228 representative rivers worldwide (Fig. 5). For lower-order rivers, such as second, third, and fourth orders, the values of $R_r(\omega)$ and $R_d(\omega)$ for different rivers show minimal variation, remaining within a narrow range (Fig. 5a and Fig. 5b). However, as river grade increases, the runoff ratios for higher-order rivers exhibit greater statistical dispersion. Overall, the mean value of $R_r(\omega)$ hovers around 0.5, fluctuating between 0.25 and 0.75, while the mean value of $R_d(\omega)$ is approximately 4, typically ranging from 3 to 5. Notably, at $\omega = 2$, $R_r(\omega)$ is smaller compared to other grades, while $R_d(\omega)$ is relatively larger. The distributions of $\tilde{R}_r$ and $\tilde{R}_d$ derived from the fitting method are relatively dense, though a few outliers exist (Fig. 5c and Fig. 5d). In general, the mean of $\tilde{R}_r$ is around 0.5, fluctuating between 0.3 and 0.6, while the mean of $\tilde{R}_d$ is about 4, maintaining a range from 3 to 5. Inspection of the regression diagnostics indicates that the estimated scaling ratios ($\tilde{R}_r$ and $\tilde{R}_d$) are sensitive to the high-magnitude fluxes characteristic of higher-order streams. Despite this variability, the log-linear regressions for the entire dataset demonstrated strong statistical significance. For $\tilde{R}_r$, the normalized runoff across different watersheds remains consistent at lower grades but exhibits significant fluctuations at higher grades, leading to increased variability in the fitted slope, which accounts for the larger fluctuations in the runoff ratio $R_r(\omega)$. In contrast, the box plots for $\tilde{R}_d$ illustrate a broader variability in discharge for higher-order rivers.

https://doi.org/10.5194/egusphere-2026-1128
Preprint. Discussion started: 6 March 2026


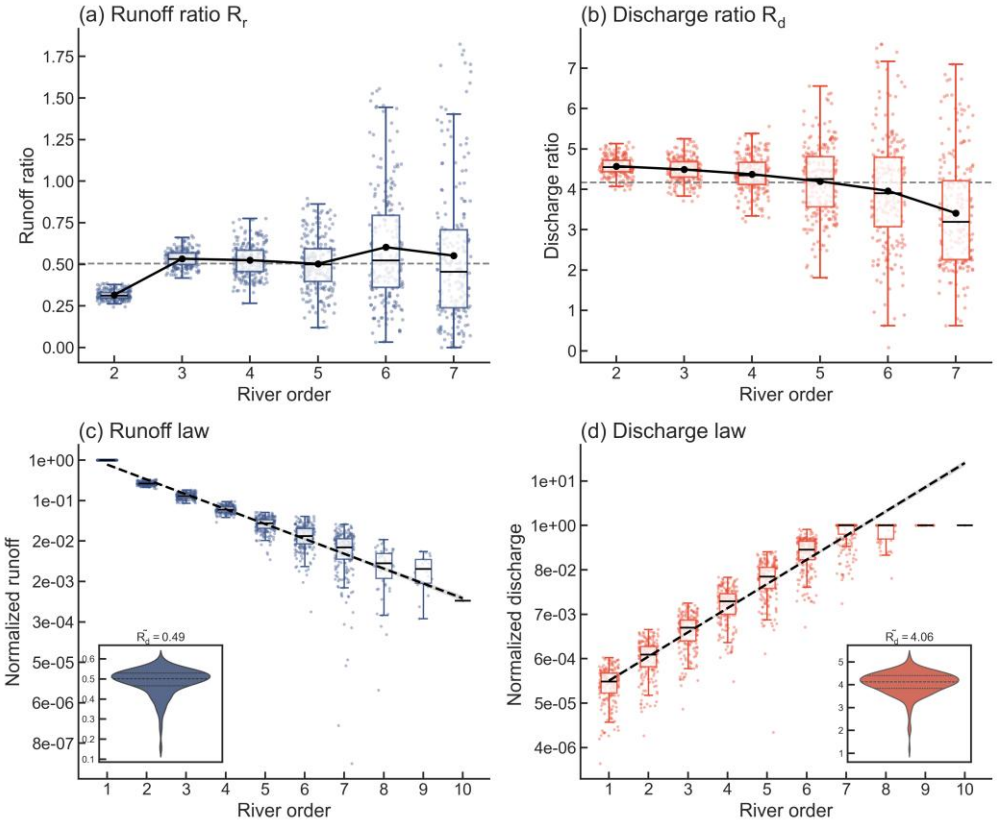


**Figure 5. Global scaling patterns of hydrological ratios across river orders. (a) Cascade runoff ratios $R_r(\omega)$ in globally representative watersheds. (b) Cascade discharge ratios $R_d(\omega)$ in globally representative watersheds. The dashed line represents the average of all runoff ratios and discharge ratios. (c) Fitting results for runoff ratios. (d) Fitting results for discharge ratios. The violin diagram in (c) and (d) presents the statistics of $e^k$, i.e., $\widetilde{R}_r$ and $\widetilde{R}_d$. Boxplots summarize the global variability at each order, where box edges define the interquartile range and central lines mark the median values.**

Further analysis of the statistical characteristics of runoff and discharge ratios considers their frequency distributions across the 228 representative rivers (Fig. 6). The calculated mean for the runoff ratio $R_r(\omega)$ is 0.52, with a standard deviation of 0.07, displaying some skewness compared to a typical normal distribution. The mean derived from the fitting method, $\tilde{R}_r$, is 0.48, with a standard deviation of 0.07, also showing skewness but with a smaller standard deviation than $R_r(\omega)$. Since $R_r(\omega)$ at $\omega = 2$ is smaller compared to other grades, this skewness is primarily driven by $R_r(2)$. Notably, this phenomenon does not appear in the runoff ratio results for other grades, particularly at $\omega = 3$, indicating that the substantial cumulative runoff from first-order rivers is the root cause. After removing $R_r(2)$, the skewness decreases, with the mean increasing to 0.56 and the standard deviation rising to 0.08. The mean for the discharge ratio $R_d(\omega)$ is 4.21, with a standard deviation of 0.40, also exhibiting skewness. The mean from the fitting method, $\tilde{R}_d$, is 4.18, with a standard deviation of 0.37, aligning closely with a

https://doi.org/10.5194/egusphere-2026-1128
Preprint. Discussion started: 6 March 2026


normal distribution. Similarly, removing $R_d(2)$ reduces the skewness, resulting in a mean of $R_d(\omega)$ decreasing to 4.14, with a standard deviation of 0.47.

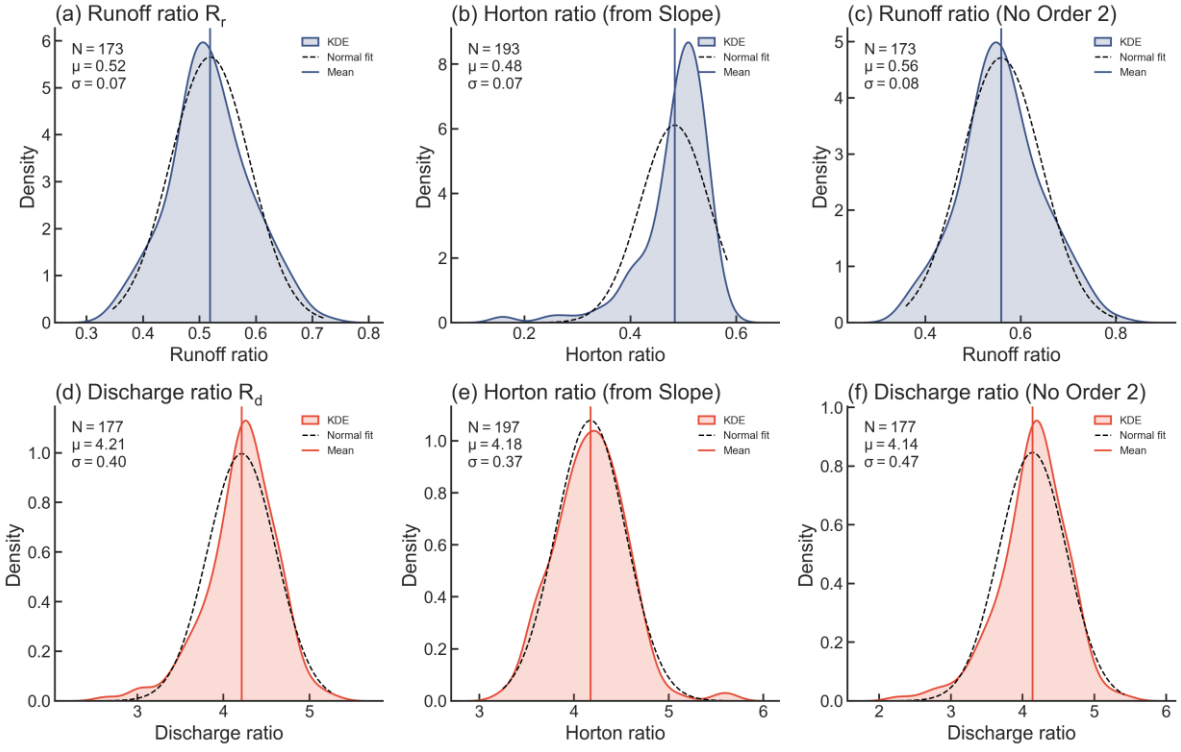


**Figure 6. Frequency distributions of Horton ratios. (a) Runoff ratio $R_r(\omega)$ frequency distribution. (b) Runoff ratio $\widetilde{R}_r$ frequency distribution. (c) Frequency distributions of $R_r(\omega)$ calculated without using order 2 runoff ratios. (d) Discharge ratio $R_d(\omega)$ frequency distribution. (e) Discharge ratio $\widetilde{R}_d$ frequency distribution. (f) Frequency distributions of $R_d(\omega)$ calculated without using order 2 runoff ratios. The runoff ratios $R_r(\omega)$ and discharge ratios $R_d(\omega)$ in (a)(c)(d)(f) are calculated by averaging the values for the different orders in each basin. The vertical line represents the mean.**

### 3.2 Relationship between runoff, discharge, and characteristic lengths of basic units in river networks

Previous studies have indicated that if rivers exhibit self-similarity during random iterations, the ratios of the iterators and the lengths of the iterators follow a geometric distribution (Mantilla et al., 2010). We can examine whether cumulative runoff and discharge exhibit proportional distribution characteristics. This relationship can be validated using the method of maximum likelihood estimation. A similar analysis can be conducted for $R_r^{out}(\lambda)$ and $R_r^{in}(\lambda)$.

The average runoff and discharge of basic units with varying characteristic lengths and inner and outer attributes were analysed for 228 representative rivers worldwide. Due to the limited number of basic units with larger characteristic lengths (those exceeding 20 represent less than 1 % of the total), which are significantly influenced by topography and exhibit high variability, our analysis focused on basic units with characteristic lengths between 1 and 20. The fitting results indicate a strong linear relationship (mean $R^2 > 0.90$) between the average runoff and discharge of these units and their characteristic lengths, with the slope distribution displaying concentrated statistical characteristics (Fig. 7).

https://doi.org/10.5194/egusphere-2026-1128
Preprint. Discussion started: 6 March 2026


Comparing the fitting results for $R(\lambda)$ and $D(\lambda)$ reveals that $k_r$ is concentrated around 1, exhibiting pronounced skewness, while $k_d$ is symmetrically distributed around 0.7. Further differentiation of basic units based on their inner and outer attributes indicates distinct topological behaviours. For inner units, the statistics for $R^{in}(\lambda)$ aligns closely with the global trend, whereas the $D^{in}(\lambda)$ is notably lower than the global average. Specifically, $k_r^{in}$ is similarly concentrated around 1 and shows skewness, whereas $k_d^{in}$ is symmetrically distributed around 0.5. In contrast, the fitting results for outer units, $R^{out}(\lambda)$ and $D^{out}(\lambda)$, align closely with the statistics for $R(\lambda)$ and $D(\lambda)$. $k_r^{out}$ maintains a high mean of 0.90, only slightly lower than that of inner units. Most notably, the mean discharge slope for outer units surpasses both the global and inner unit slopes, suggesting that headwater or exterior links accumulate discharge more efficiently relative to their characteristic length.

The frequency distributions of the scaling slopes reveal distinct topological behaviours between runoff and discharge (Fig. 8). For runoff, the distributions of $k_r$ and $k_r^{in}$ are highly consistent, displaying strong skewness and concentrating around a mean of 0.95 ($\sigma = 0.10$). While $k_r^{out}$ is relatively more dispersed ($\sigma = 0.16$), its mean remains high at 0.89, only slightly lower than that of inner units. This suggests that runoff generation is topologically robust, maintaining high accumulation efficiency across both internal and external links despite greater geometric variability in outer regions.

In contrast, the discharge scaling exhibits a significant topological divergence. The distribution of $k_d$ is less concentrated than $k_r$ but demonstrates stronger normality. Most notably, the mean discharge slope for outer units ($k_d^{out} = 0.79$) significantly surpasses that of inner units ($k_d^{in} = 0.54$). This indicates a functional separation: outer units, acting as headwater collectors, accumulate discharge efficiently relative to their length. Conversely, inner units function primarily as transmission corridors where discharge accumulation slows down. Furthermore, the universal observation that $k_d < k_r$ confirms that across all scales, runoff volume scales more rapidly with characteristic length than peak discharge, reflecting the attenuation effects of channel routing.

https://doi.org/10.5194/egusphere-2026-1128
Preprint. Discussion started: 6 March 2026


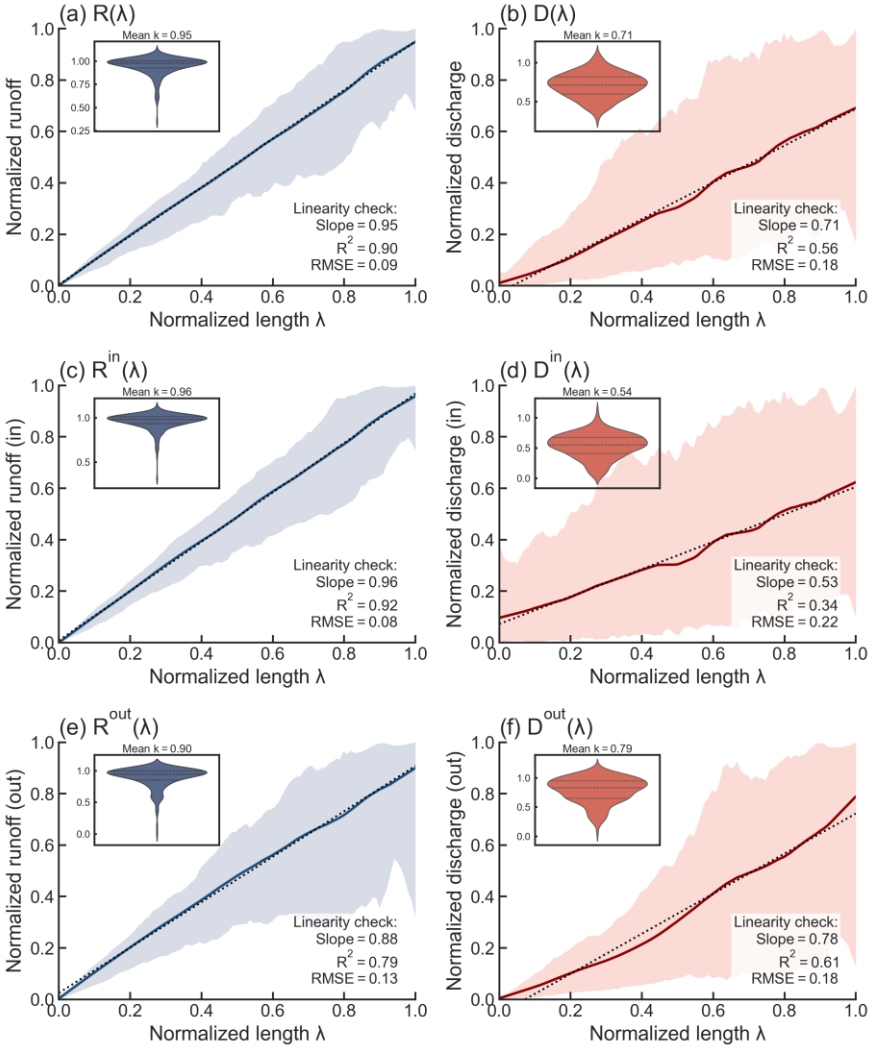


**Figure 7. Universal linear scaling of normalized hydrological functions across basic units. Panels (a) to (f) present the linear fitting results for $R(\lambda)$, $D(\lambda)$, $R^{in}(\lambda)$, $D^{in}(\lambda)$, $R^{out}(\lambda)$, and $D^{out}(\lambda)$, along with the corresponding statistical results for $k_r$, $k_d$, $k_r^{in}$, $k_d^{in}$, $k_r^{out}$, and $k_d^{out}$. Data are presented as statistical aggregates: solid curves represent the global mean trends, while shaded regions indicate the variability range. Inset violin plots display the probability density distributions of the fitted slopes for individual rivers. Quantitative metrics in the bottom right of each panel verify the robustness of the linear scaling laws.**

https://doi.org/10.5194/egusphere-2026-1128
Preprint. Discussion started: 6 March 2026


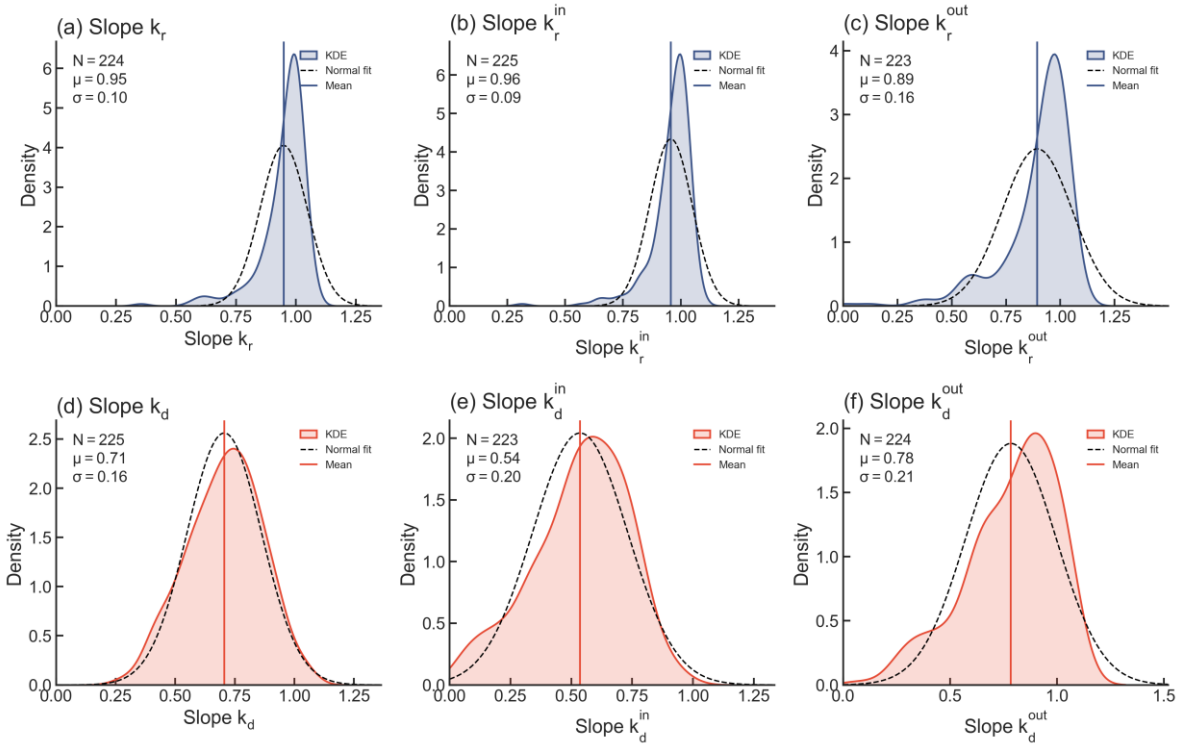


**Figure 8. Frequency distributions of the scaling slopes. Panels (a) to (f) depict the frequency distributions of the scaling slopes $k_r$, $k_r^{in}$, $k_r^{out}$, $k_d$, $k_d^{in}$, and $k_d^{out}$ derived from Figure 7.**

### 3.3 Statistical patterns of runoff ratios and discharge ratios in basic units

The runoff ratios and discharge ratios of inner and outer links within river basic units approximately follow a log-normal distribution, specifically, $ln(R_r^{unit}) \sim N(\mu_r, \sigma_r^2)$, $ln(R_d^{unit}) \sim N(\mu_d, \sigma_d^2)$. Utilizing maximum likelihood estimation for 228 representative rivers worldwide, the expected values and confidence interval widths for the distribution of parameters across different basic units were calculated (Fig. 9). Statistical analysis reveals that the parameters of the basic units, including the unit runoff ratio $R_r^{unit}$, unit discharge ratio $R_d^{unit}$, inner unit runoff ratio $R_r^{unit\_in}$, inner unit discharge ratio $R_d^{unit\_in}$, outer unit runoff ratio $R_r^{unit\_out}$, and outer unit discharge ratio $R_d^{unit\_out}$, all approximate a log-normal distribution: $ln(R^{unit}) \sim N(\mu, \sigma^2)$. The expected value of $R_r^{unit}$ ranges from 0.79 to 1.41, with a 95 % confidence interval of 0 to 0.11. The expected value of $R_d^{unit}$ spans from 0.65 to 2.33, with a 95 % confidence interval of 0.01 to 0.32. For $R_r^{unit\_in}$, the expected value ranges from 0.69 to 0.97, with a 95 % confidence interval of 0 to 0.12. The expected value for $R_d^{unit\_in}$ varies from 0.29 to 2.96, with a 95 % confidence interval of 0.02 to 0.70. The expected value of $R_r^{unit\_out}$ ranges from 0.96 to 1.89, with a 95 % confidence interval of 0 to 0.34. Lastly, the expected value for $R_d^{unit\_out}$ spans from 0.69 to 1.03, with a 95 % confidence interval of 0 to 0.25. Notably, for most parameters of the basic units, the expected values are closely aligned across different rivers, and the widths of the confidence intervals are relatively narrow, indicating a high degree of reliability in the results. A comparison of the

https://doi.org/10.5194/egusphere-2026-1128
Preprint. Discussion started: 6 March 2026


runoff and discharge ratios between inner and outer units reveals that the ratios for outer units are consistently higher than those for inner units across various watersheds.

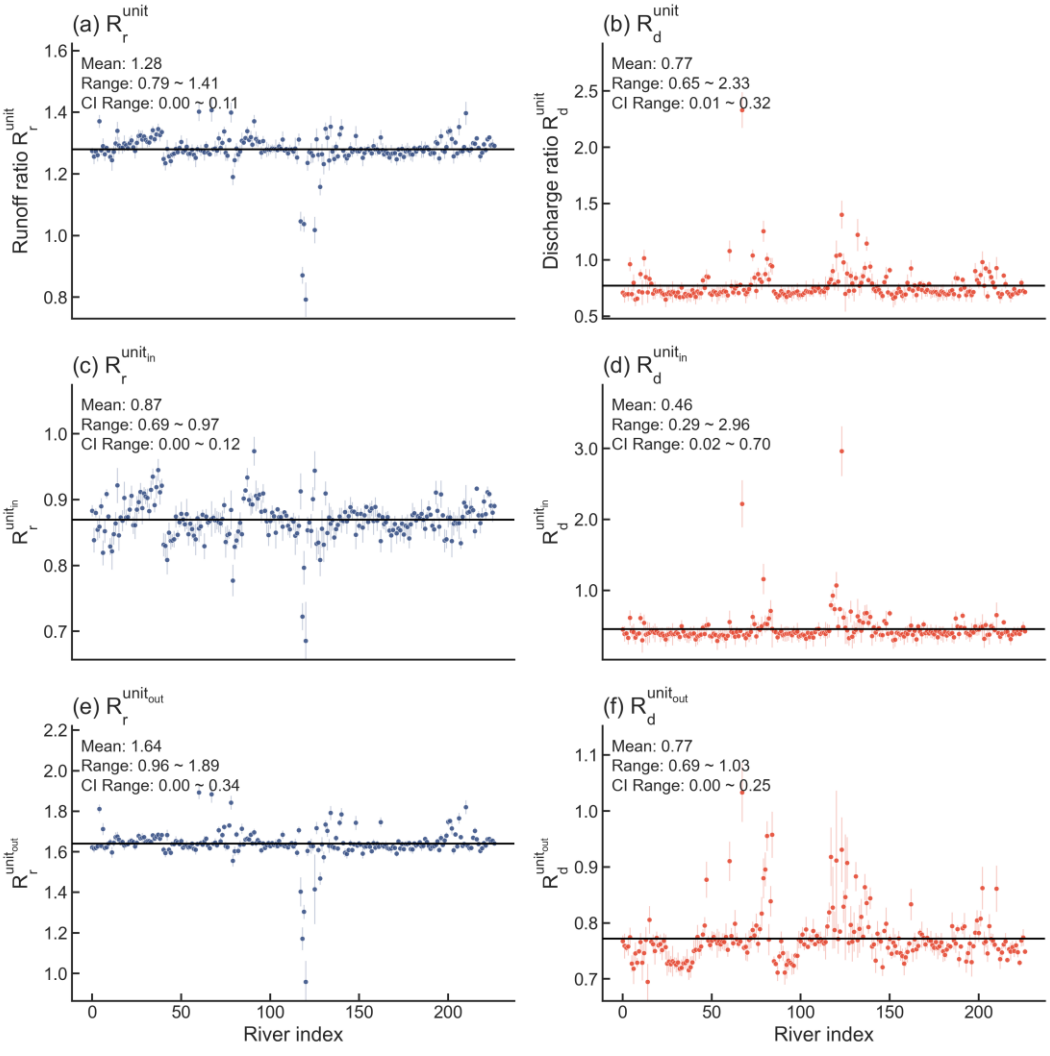


**Figure 9. Statistical invariance of basic unit characteristic parameters. Panels (a) to (f) show the expected means for the parameters of representative river basic units: $R_r^{unit}$, $R_d^{unit}$, $R_r^{unit\_in}$, $R_d^{unit\_in}$, $R_r^{unit\_out}$, and $R_d^{unit\_out}$. The lines on either side of each point represent the width of the 95 % confidence interval. The horizontal line indicates the global ensemble mean.**

Further statistical analysis of the frequency distribution of expected values for the parameters of basic units in representative rivers was conducted (Fig. 10). The mean of $R_r^{unit}$ is 1.28, situated between the mean of $R_r^{unit\_in}$ at 0.87 and the mean of $R_r^{unit\_out}$ at 1.64. Similarly, the mean of $R_d^{unit}$ is 0.76, positioned between the mean of $R_d^{unit\_in}$ at 0.44 and the mean of $R_d^{unit\_out}$ at 0.77. The smaller standard deviations indicate that the distribution of expected means is concentrated, demonstrating analogous characteristics for both runoff ratios and discharge ratios. Notably, the distribution of expected values for discharge ratios exhibits greater skewness compared to that of runoff ratios.

https://doi.org/10.5194/egusphere-2026-1128
Preprint. Discussion started: 6 March 2026


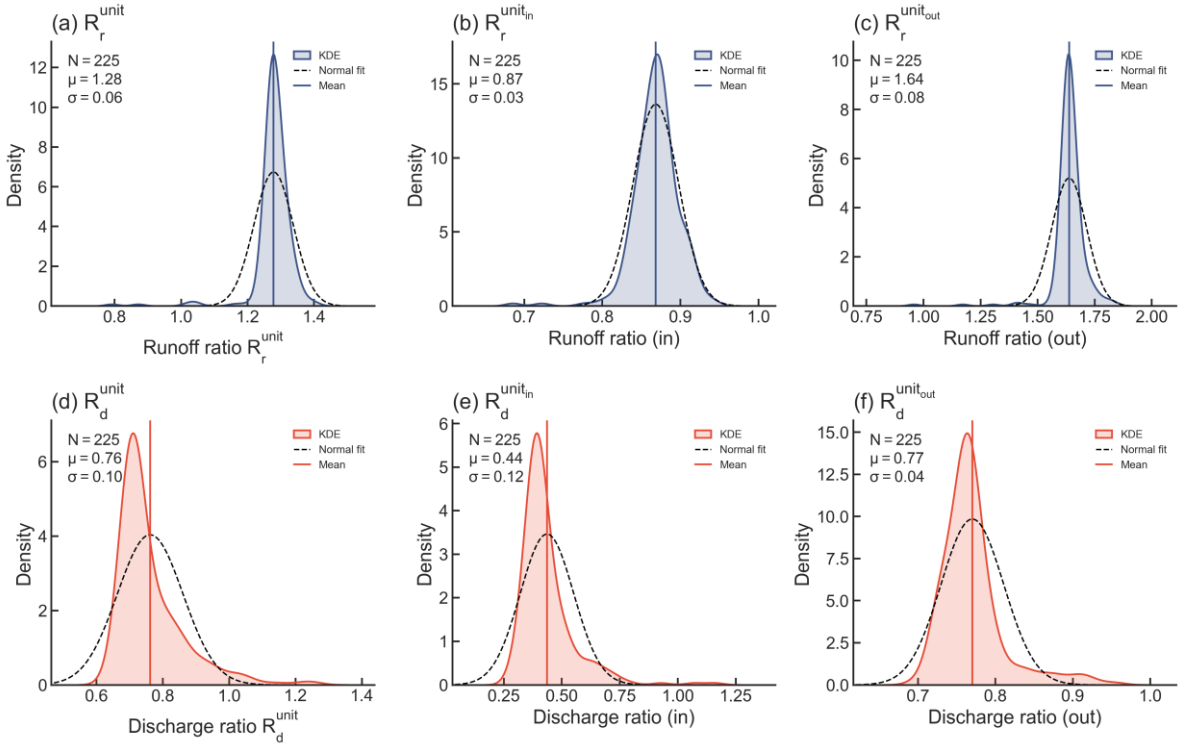


**Figure 10. Global probability distributions of basic unit parameters. Panels (a) to (f) depict the frequency distributions of the expected means for $R_r^{unit}$, $R_d^{unit}$, $R_r^{unit\_in}$, $R_d^{unit\_in}$, $R_r^{unit\_out}$, and $R_d^{unit\_out}$.**

## 4 Discussion

Collectively, our findings suggest that global river network topology imposes a unified, scale-invariant constraint on hydrological response dynamics. This consistency is evident across various scales, variables, and hierarchies, reflecting the coherence of river network structures.

### 4.1 Hydrological characteristics in the perspective of H–S ordering method

The H–S ordering method provides an intuitive and systematic framework for understanding the variations in hydrological characteristics among different river classes. The invariance of runoff and discharge ratios validates the effectiveness of the conventional H–S ordering method in describing hydrological hierarchical features (Bai et al., 2015b). However, in higher-order rivers, the cumulative characteristics of runoff and discharge, along with the influence of geomorphology, increase the variability of these ratios. Consequently, the H–S ordering method may not fully capture localized variations within complex river systems.

Notably, first-order rivers exhibit significantly inflated cumulative runoff. This phenomenon cannot be attributed solely to external climatic forcing (e.g., precipitation heterogeneity); rather, it likely reflects intrinsic structural controls inherent to the

https://doi.org/10.5194/egusphere-2026-1128
Preprint. Discussion started: 6 March 2026


network topology, specifically the dominance of source-area contributions in headwater catchments. As source rivers with relatively small watershed areas, their runoff is predominantly derived from local precipitation and surface runoff, making them particularly susceptible to the uneven distribution of topography and precipitation (Pelletier, 2013). Additionally, the pronounced runoff in first-order rivers may also be influenced by the methods used for river network extraction. Beyond potential DEM resolution sensitivity, this deviation in first-order streams likely reflects the physical "hillslope-to-channel" transition threshold (Montgomery and Dietrich, 1992). In these source areas, hydrological response is dominated by hillslope processes rather than the channelized network topology that governs higher-order streams, resulting in a distinct scaling regime (Perron et al., 2012; Passalacqua et al., 2015). Future studies could further validate these findings using more refined hydrological models and high-resolution river network data.

Moreover, the hydrological characteristics from the perspective of river network classification can also be correlated with geomorphological features. For the runoff ratio, the long-term average runoff depth for a region can be expressed through the runoff coefficient and average precipitation. Given that the distribution of different river segments across various classes within a watershed is relatively uniform, we can hypothesize that the average runoff coefficients $\bar{\alpha}$ and average precipitation $\bar{P}$ for rivers of different classes are approximately equal. Consequently, the runoff ratio can be expressed in terms of the branch ratio $R_B(\omega)$ and the confluence area ratio $R_C(\omega)$ as follows Eq. (8):

$$R_r(\omega) = \frac{\sum r_\omega}{\sum r_{\omega-1}} \propto \frac{N_\omega}{N_{\omega-1}} \times \frac{C_\omega}{C_{\omega-1}} \times \frac{\bar{\alpha}_\omega}{\bar{\alpha}_{\omega-1}} \times \frac{\bar{P}_\omega}{\bar{P}_{\omega-1}} \propto \frac{1}{R_B(\omega)} \times R_C(\omega)\ , \tag{8}$$

Similarly, for discharge ratios, it can be posited that the ratio of the long-term average discharge at the outlets of different class watersheds is approximately equal to the watershed area ratio $R_A(\omega)$ as follows Eq. (9):

$$\mathrm{R_d}(\omega) = \frac{\bar{\mathrm{d}}_\omega}{\bar{\mathrm{d}}_{\omega-1}} \propto \frac{\sum \mathrm{d}_\omega}{\mathrm{N}_\omega} \Big/ \frac{\sum \mathrm{d}_{\omega-1}}{\mathrm{N}_{\omega-1}} \propto \frac{\mathrm{N}_{\omega-1}}{\mathrm{N}_\omega} \times \frac{\mathrm{N}_\omega}{\mathrm{N}_{\omega-1}} \times \frac{\bar{\mathrm{A}}_\omega}{\bar{\mathrm{A}}_{\omega-1}} \propto \mathrm{R_A}(\omega)\ , \tag{9}$$

Overall, there exists a strong linear correlation between the runoff ratio $R_r$ and the ratio $R_C/R_B$, as well as between the discharge ratio $R_d$ and the area ratio $R_A$ (Fig. 11). The observed data points cluster tightly around the theoretical 1:1 reference line, indicating that the hierarchical hydrological features at the traditional H–S classification scale can be directly related to the hierarchical geomorphological characteristics. Specifically, this alignment confirms that hydrological transport is primarily topologically controlled (Rodriguez-Iturbe and Rinaldo, 1997; Banavar et al., 1999). The observed slight deviation from unity likely reflects secondary transmission losses and evaporation, particularly in higher-order streams; yet, the dominance of geometric scaling underscores how the river network's fractal structure fundamentally constrains hydrological fluxes (Tarboton, 1996).

https://doi.org/10.5194/egusphere-2026-1128
Preprint. Discussion started: 6 March 2026


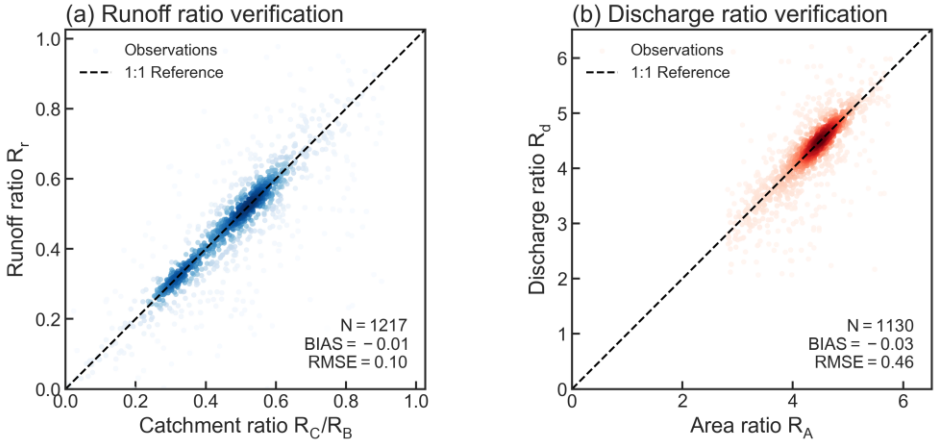


**Figure 11. Macro-scale verification of hydrological scaling laws. (a) Verification scatter plot of $R_r$ versus $R_C/R_B$. (b) Verification scatter plot of $R_d$ versus $R_A$. The dashed line represents the theoretical 1:1 reference.**

### 4.2 Transition from H–S ordering method to river network pyramid

The shift from the traditional H–S ordering method to the river network pyramid model represents not only a reclassification of river hierarchies but also reveals the transitional relationships in hydrological characteristics between different levels within river networks. This transition moves the description of river network structures from hierarchical features to hierarchical attributes. Compared to the river classifications obtained through the H–S method, the river characteristic lengths derived from the S–S method provide a richer description of the topological information of river networks, offering deeper insights into the hydrological behaviour of river basins.

The relationship between characteristic length and hydrological features illustrates the transition patterns between trunk streams and tributaries within river systems. As the characteristic length increases, the hydrological features of basic units gradually change, reflecting a balance and transition from localized to holistic hydrological processes. Basic units with shorter characteristic lengths typically represent smaller tributaries, which exhibit more consistent hydrological characteristics. In contrast, basic units with longer characteristic lengths represent trunk streams or larger river sections, where regional differences become more pronounced due to the larger watershed sizes and drainage areas.

It is noteworthy that the observed mean trends for both hydrological variables generally follow the theoretical linear reference (Fig. 12), further validating the rationale of the river network pyramid model. Specifically, the normalized runoff demonstrates a remarkably strict linear accumulation with minimal deviation, indicating a highly uniform scaling process. While the discharge also adheres to the global linear trend, it exhibits relatively higher variability compared to runoff. This alignment indicates that as the analysis transitions from the macro-scale H–S classification to the micro-scale of basic units, the hydrological features accumulate along the characteristic length according to a stable topological law. Rather than being distorted by complex non-linear processes, the hydrological response maintains a predictable progression within these fundamental units.

https://doi.org/10.5194/egusphere-2026-1128
Preprint. Discussion started: 6 March 2026


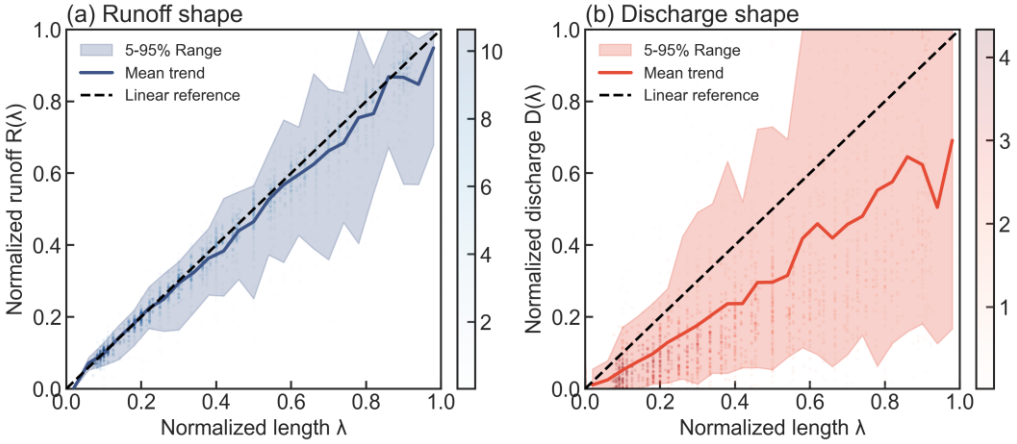


**Figure 12. Relationship between normalized hydrological variables and characteristic length. (a) Normalized runoff $R(\lambda)$ versus normalized length $\lambda$. (b) Normalized discharge $D(\lambda)$ versus normalized length $\lambda$.**

### 4.3 Characteristics of basic units in the river network pyramid

The basic units within the river network pyramid model provide a novel understanding of the hierarchical structure of river systems. Each basic unit encompasses both internal and external link units, where the former represents sections closer to the river trunk, while the latter denotes smaller tributaries or upstream segments of those tributaries. In our study of 228 representative rivers, we found that both the runoff ratios and flow ratios of these basic units approximately follow a log-normal distribution, indicating inherent statistical regularity.

For internal and external units, the expected mean values of the runoff and flow ratios for most rivers are distributed within a narrow range, reflecting the relative consistency and reliability of these parameters on a global scale. The observed phenomenon that external units generally exhibit higher runoff and flow ratios than internal units highlights the differences in hydrological characteristics between these two types of units. This suggests that in external units, the hydrological processes influenced by the branching areas are relatively stronger, whereas in internal units, the hydrological processes in the trunk regions exert a more dominant influence.

From the perspective of basic units, the relationship between hydrological characteristics and geometric features reveals a fundamental topological decoupling (Fig. 13). Unlike the strong linear coupling observed at the macro-scale, the direct correlation between unit hydrological ratios and geometric ratios is virtually non-existent. Instead, the hydrological ratios maintain a statistically constant mean value, independent of the unit's local geometric magnitude. This indicates that at the finest topological resolution, hydrological efficiency becomes an intrinsic property, independent of the unit's local geometric magnitude. The local topographical features and spatial variability act as high-frequency noise that is effectively filtered out by the network topology. Consequently, while the distributions of runoff and flow ratios exhibit statistical consistency (log-normal), their individual values do not linearly scale with area or count. This narrow distribution of hydrological parameters, contrasted with the broad variability of geometric parameters, confirms that basic units function as standardised topological

https://doi.org/10.5194/egusphere-2026-1128
Preprint. Discussion started: 6 March 2026


modules. They impose a unified, scale-invariant constraint on hydrological response, ensuring global stability despite local geometric heterogeneity.

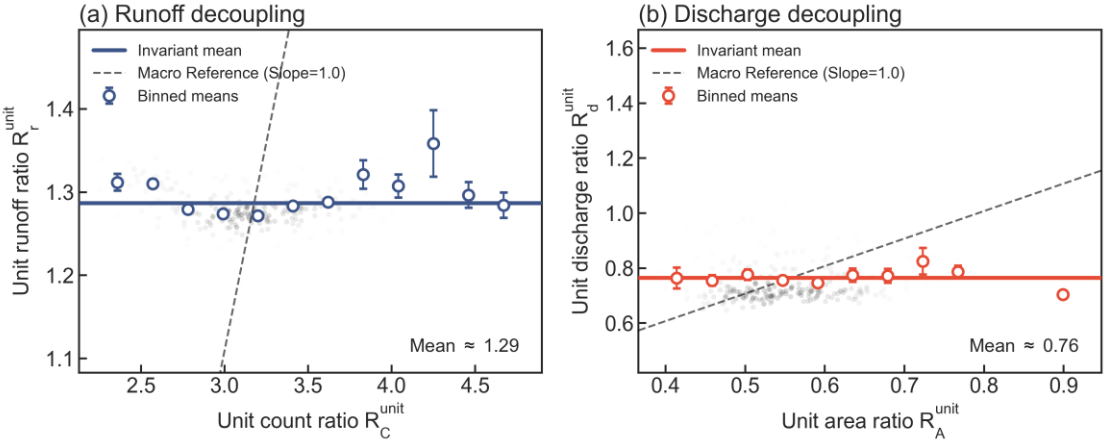


**Figure 13. Topological decoupling of hydrological functions at the basic unit scale. (a) Relationship between $R_d^{unit}$ and $R_A^{unit}$. (b) Relationship between $R_d^{unit}$ and $R_C^{unit}$.**

### 4.4 Correlation and consistency across different scales

As a typical natural fractal structure, the river network system should exhibit its self-similarity through consistent characteristics across different analytical frameworks. Through a comprehensive examination of the H–S ordering system, the river network pyramid model, and the basic unit levels, we observed similarities in the statistical characteristics of key hydrological parameters. Although these analytical frameworks adopt different perspectives, they reveal a common pattern in river network structures, suggesting that river network morphology may be governed by the same self-organizing principles (Rinaldo et al., 2014).

Notably, the runoff ratio and discharge ratio – two key hydrological parameters discussed in the previous sections—exhibit significant statistical regularity at their respective scales. The runoff ratio reflects the distribution characteristics of water sources, while the flow ratio characterizes the efficiency of water flow transmission. Both parameters demonstrate similar concentrated distribution characteristics across the three analytical frameworks, indicating that the self-similarity of river networks encompasses not only geometric forms but also functional attributes. This observation aligns with Mandelbrot's fractal theory (Zhang et al., 2009), supporting the understanding of river networks as self-organizing systems that unify structure and function.

Through the analysis of 228 representative rivers, we found that the characteristics at these different scale frameworks may point to two important phenomena: first, scale robustness in parameter distribution, reflected in similar statistical characteristics across scales; and second, the potential intrinsic connections among these features, demonstrated by the similar hydrological patterns captured by different analytical methods. Together, these aspects form the basis for studying the self-similarity of river networks, supporting the scientific view of river networks as natural fractal systems.

https://doi.org/10.5194/egusphere-2026-1128
Preprint. Discussion started: 6 March 2026


To explicitly test the robustness of these topological patterns against climatic forcing, we performed a stratified analysis partitioning global basins into humid and arid regimes based on the HydroATLAS aridity index. The results reveal a remarkable consistency across scales (Fig. 14).

At the macro-scale, the scaling behaviour of the runoff ratio $R_r$ remains structurally identical across climate zones, with both regimes exhibiting a similar upward trend with increasing stream order (Fig. 14a). While the discharge ratio $R_d$ also shows high congruence at lower orders, a divergence appears in higher-order streams, where arid basins exhibit lower values (Fig. 14b). This deviation physically manifests the non-linear transmission losses (e.g., evaporation and infiltration) characteristic of dryland rivers, yet the persistence of the power-law scaling underscores the primacy of network topology in constraining hydrological fluxes.

Most critically, at the micro-scale of basic units, the hydrological self-similarity proves to be strictly invariant. The distribution of unit runoff ratios $R^{unit}$ for humid and arid regions is statistically indistinguishable, with overlapping interquartile ranges (Fig. 14c). This suggests that the fundamental building blocks of hydrological response are universally constrained by network geometry, acting as a low-pass filter that smooths out high-frequency climatic variability to produce unified global scaling laws (Seybold et al., 2017; Banavar et al., 1999). This empirical universality finds a rigorous theoretical basis in stochastic network theory, which predicts that the ensemble statistics of Horton ratios converge to stable distributions regardless of local geometric variation (Wang and Waymire, 1991). Furthermore, generalized ordering frameworks demonstrate that the hierarchical backbone of river networks remains topologically robust even in the presence of reticulate loops or anthropogenic regulation (Mileyko et al., 2012). Thus, local perturbations – whether climatic, anthropogenic, or geometric—act merely as second-order fluctuations that do not dismantle the primary topological constraints governing global hydrological scaling.

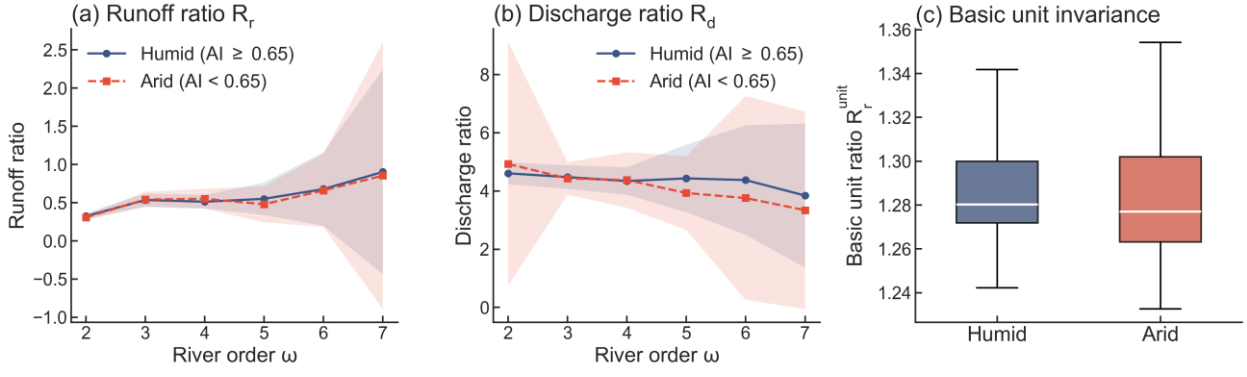


**Figure 14. Climatic invariance of hydrological topology across global river networks. (a) Scaling of Runoff Ratio $R_r$ versus river order for humid and arid basins. (b) Scaling of Discharge Ratio $R_d$ versus river order. Shaded bands in (a) and (b) represent the standard deviation. (c) Boxplots of $R^{unit}$ comparisons under different climatic conditions. The classification is based on the HydroATLAS aridity Index with a threshold of 0.65.**

Particularly, this potential self-similarity is especially evident in the hydrological-geomorphological coupling relationships. The connections between hydrological characteristics and geomorphological features discussed in previous sections, though expressed differently, all point to an optimized relationship between river network structure and water flow transmission

https://doi.org/10.5194/egusphere-2026-1128
Preprint. Discussion started: 6 March 2026


(Różycka and Migoń, 2021). This observed optimization trend across different scales suggests that river network morphology may adhere to certain scale-invariant physical principles.

## 5 Conclusions

This study quantifies the universal hydrological patterns of global river networks by integrating the classical Horton–Strahler framework with a hierarchical pyramid decomposition technique. By analysing 228 representative basins spanning diverse hydro-climatic regimes, we reveal that global river network topology imposes a unified, scale-invariant constraint on hydrological response dynamics. The main conclusions are drawn as follows:

First, while the traditional Horton–Strahler ordering method effectively captures macro-scale hydrological hierarchical features, it exhibits significant deviations in headwater catchments (first-order rivers). This deviation reflects the physical hillslope-to-channel transition, highlighting the limitations of macro-scale classifications in fully capturing localized variations within complex river systems.

Second, the transition to the river network pyramid model, characterized by the characteristic length, reveals a strict linear accumulation of hydrological features. Rather than being distorted by complex non-linear processes, the hydrological response maintains a stable and predictable progression within these fundamental topological units.

Third, at the micro-scale of basic units, we discovered a fundamental topological decoupling. The runoff and discharge ratios of basic units maintain a statistically constant mean value (approximately following a log-normal distribution), independent of the unit's local geometric magnitude. Crucially, this topological invariance holds true across contrasting climatic regimes (humid versus arid). This demonstrates that river network topology functions as a geomorphic low-pass filter, effectively damping high-frequency climatic and spatial variability to produce unified global scaling laws.

Beyond theoretical insights into the self-similarity of natural fractal systems, these findings carry significant practical implications. The identified universal scaling ratios offer physics-informed priors for next-generation hydrological modelling. They provide critical constraints for scale-aware parameterization in macro-scale models and can potentially aid in the upscaling of runoff-routing schemes (Thober et al., 2019). Furthermore, as deep learning approaches such as RiverMamba become increasingly dominant in global discharge forecasting (Hakam Shams Eddin et al., 2025), our findings on unit-level topological invariance offer a physically interpretable metric for validating the structural realism of synthetic networks generated by these AI models. Integrating such topological laws will help bridge the gap between data-driven predictions and physical consistency in ungauged basins.

https://doi.org/10.5194/egusphere-2026-1128
Preprint. Discussion started: 6 March 2026


## 2 Appendices

All material required to understand the essential aspects of the manuscript such as experimental methods, data, and interpretation should preferably be included in the main text. Additional figures, tables, as well as technical and theoretical developments which are not critical to support the conclusion of the manuscript, but which provide extra detail and/or support useful for experts in the field and whose inclusion in the main text would disrupt the flow of descriptions or demonstrations may be presented as appendices. These should be labelled with capital letters: Appendix A, Appendix B etc. Equations, figures, and tables should be numbered as (A1), Fig. B5, or Table C6, respectively. Please keep in mind that appendices are part of the manuscript whereas supplements (see below) are published along with the preprint or journal article.

## Code and Data availability

The river network and hydro-environmental attribute data used in this study are available from the HydroSHEDS project. Specifically, we utilized the BasinATLAS and RiverATLAS datasets (version 1.0) provided by HydroATLAS. The data are publicly available at https://www.hydrosheds.org/page/hydroatlas. The code used for data processing and statistical analysis in this study is available from the corresponding author upon reasonable request.

## Author contributions

DZ and CZ conceptualised the study and designed the methodology. CZ performed the primary data processing, conducted the formal analysis, and wrote the original manuscript draft. QK, YC, SL, and RW assisted with spatial data curation and database management. DX, JW, and JH contributed to the computational coding and data validation. QZ, JG, and JL assisted with data visualisation and theoretical discussions. GW and DZ supervised the project and provided critical feedback. CZ and DZ revised the manuscript with contributions from all co-authors.

## Competing interests

The authors declare that they have no conflict of interest.

## Acknowledgements

The authors gratefully acknowledge the State Key Laboratory of Hydroscience and Engineering at Tsinghua University and Qinghai University for providing the essential research facilities and computational infrastructure. We also extend our sincere gratitude to the developers and maintainers of the globally open-source databases, particularly the HydroATLAS and DMP datasets, which provided the foundational global river network and hydrological data that made this study possible.

https://doi.org/10.5194/egusphere-2026-1128
Preprint. Discussion started: 6 March 2026


**Financial support**

This research has been supported by the major science and technology projects in Qinghai Province (grant no. 2024-GX-A3) and the State Key Laboratory of Hydroscience and Engineering (grant no. sklhse-TD-2024-F01).

**References**

Bai, R.: Large Scale Drainage Network Extraction and River Structure Rules, Ph.D, Tsinghua, Beijing (in chinese), 157 pp., 2015.

Bai, R., Tiejian, L., Huang, Y., Jiaye, L., and Wang, G.: An efficient and comprehensive method for drainage network extraction from DEM with billions of pixels using a size-balanced binary search tree, Geomorphology, 238, 56-67, https://doi.org/10.1016/j.geomorph.2015.02.028, 2015a.

Bai, R., Tiejian, L., Huang, Y., Jiaye, L., Wang, G., and Yin, D.: A hierarchical pyramid method for managing large-scale high-resolution drainage networks extracted from DEM, Computers & Geosciences, 85, 234-247, https://doi.org/10.1016/j.cageo.2015.06.019, 2015b.

Banavar, J. R., Maritan, A., and Rinaldo, A.: Size and form in efficient transportation networks, Nature, 399, 130-132, https://doi.org/10.1038/20144, 1999.

Bogale, A.: Morphometric analysis of a drainage basin using geographical information system in Gilgel Abay watershed, Lake Tana Basin, upper Blue Nile Basin, Ethiopia, Applied Water Science, 11, 122, https://doi.org/10.1007/s13201-021-01447-9, 2021.

Czuba, J. A. and Foufoula-Georgiou, E.: Dynamic connectivity in a fluvial network for identifying hotspots of geomorphic change, Water Resour. Res., 51, 1401-1421, https://doi.org/10.1002/2014WR016139, 2015.

Demarchi, L., Bizzi, S., and Piégay, H.: Regional hydromorphological characterization with continuous and automated remote sensing analysis based on VHR imagery and low-resolution LiDAR data, Earth Surface Processes and Landforms, 42, 531-551, https://doi.org/10.1002/esp.4092, 2017.

Dodds, P. S. and Rothman, D. H.: Geometry of river networks. II. Distributions of component size and number, Physical Review E, 63, 016116, https://doi.org/10.1103/PhysRevE.63.016116, 2000a.

Dodds, P. S. and Rothman, D. H.: Scaling, universality, and geomorphology, Annual Review of Earth and Planetary Sciences, 28, 571-610, https://doi.org/10.1146/annurev.earth.28.1.571, 2000b.

Dodds, P. S. and Rothman, D. H.: Geometry of river networks. III. Characterization of component connectivity, Physical Review E, 63, 016117, https://doi.org/10.1103/PhysRevE.63.016117, 2000c.

Döll, P., Kaspar, F., and Lehner, B.: A global hydrological model for deriving water availability indicators: model tuning and validation, Journal of Hydrology, 270, 105-134, https://doi.org/10.1016/S0022-1694(02)00283-4, 2003.

Farr, T. G., Rosen, P. A., Caro, E., Crippen, R., Duren, R., Hensley, S., Kobrick, M., Paller, M., Rodriguez, E., and Roth, L.: The shuttle radar topography mission, Reviews of geophysics, 45, https://doi.org/10.1029/2005RG000183, 2007.

Fekete, B. M., Vörösmarty, C. J., and Lammers, R. B.: Scaling gridded river networks for macroscale hydrology: Development, analysis, and control of error, Water Resour. Res., 37, 1955-1967, https://doi.org/10.1029/2001WR900024, 2001.

Gong, J. and Xie, J.: Extraction of drainage networks from large terrain datasets using high throughput computing, Computers & Geosciences, 35, 337-346, https://doi.org/10.1016/j.cageo.2008.09.002, 2009.

Güneralp, İ., Abad, J. D., Zolezzi, G., and Hooke, J.: Advances and challenges in meandering channels research, Geomorphology, 163, 1-9, https://doi.org/10.1016/j.geomorph.2012.04.011, 2012.

Gurnell, A., Rinaldi, M., Belletti, B., Bizzi, S., Blamauer, B., Braca, G., Buijse, A., Bussettini, M., Camenen, B., and Comiti, F.: A multi-scale hierarchical framework for developing understanding of river behaviour to support river management, Aquatic sciences, 78, 1-16, https://doi.org/10.1007/s00027-015-0424-5, 2016.

https://doi.org/10.5194/egusphere-2026-1128
Preprint. Discussion started: 6 March 2026


Hakam Shams Eddin, M., Zhang, Y., Kollet, S., and Gall, J.: RiverMamba: A State Space Model for Global River Discharge and Flood Forecasting, arXiv e-prints, arXiv: 2505.22535, https://doi.org/10.48550/arXiv.2505.22535, 2025.

Heasley, E. L., Clifford, N. J., and Millington, J. D. A.: Integrating network topology metrics into studies of catchment-level effects on river characteristics, Hydrology and Earth System Sciences, 23, 2305-2319, https://doi.org/10.5194/hess-23-2305-2019, 2019.

Horton, R. E.: Erosional development of streams and their drainage basins; hydrophysical approach to quantitative morphology, Geological society of America bulletin, 56, 275-370, https://doi.org/10.1130/0016-7606(1945)56[275:EDOSAT]2.0.CO;2, 1945.

Hou, K., Yang, W., Sun, J., and Sun, T.: A method for extracting drainage networks with heuristic information from digital elevation models, Water Science and Technology, 64, 2316-2324, https://doi.org/10.2166/wst.2011.819, 2011.

Jaeger, K. L., Olden, J. D., and Pelland, N. A.: Climate change poised to threaten hydrologic connectivity and endemic fishes in dryland streams, Proceedings of the National Academy of Sciences, 111, 13894-13899, https://doi.org/10.1073/pnas.1320890111, 2014.

Lane, B. A., Pasternack, G. B., and Sandoval Solis, S.: Integrated analysis of flow, form, and function for river management and design testing, Ecohydrology, 11, e1969, https://doi.org/10.1002/eco.1969, 2018.

Lehner, B. and Grill, G.: Global river hydrography and network routing: baseline data and new approaches to study the world's large river systems, Hydrological Processes, 27, 2171-2186, https://doi.org/10.1002/hyp.9740, 2013.

Lehner, B., Verdin, K., and Jarvis, A.: New global hydrography derived from spaceborne elevation data, Eos, Transactions American Geophysical Union, 89, 93-94, https://doi.org/10.1029/2008EO100001, 2008.

Leopold, L., Wolman, M., and Miller, J.: Fluvial processes in geomorphology, Fluvial Processes in Geomorphology, Dover Publications, Inc., New York, NY1964.

Li, M., Seybold, H., Wu, B., Chen, Y., and Kirchner, J. W.: Interaction Between Tectonics and Climate Encoded in the Planform Geometry of Stream Networks on the Eastern Tibetan Plateau, Geophysical Research Letters, 50, https://doi.org/10.1029/2023gl104121, 2023.

Li, Z., Zhu, C., and Gold, C.: Digital terrain modeling: principles and methodology, CRC press2004.

Lindsay, J. B. and Dhun, K.: Modelling surface drainage patterns in altered landscapes using LiDAR, International Journal of Geographical Information Science, 29, 397-411, https://doi.org/10.1080/13658816.2014.975715, 2015.

Linke, S., Lehner, B., Ouellet Dallaire, C., Ariwi, J., Grill, G., Anand, M., Beames, P., Burchard-Levine, V., Maxwell, S., Moidu, H., Tan, F., and Thieme, M.: Global hydro-environmental sub-basin and river reach characteristics at high spatial resolution, Scientific Data, 6, https://doi.org/10.1038/s41597-019-0300-6, 2019.

Mantilla, R., Troutman, B. M., and Gupta, V. K.: Testing statistical self-similarity in the topology of river networks, Journal of Geophysical Research: Earth Surface, 115, https://doi.org/10.1029/2009JF001609, 2010.

Mcconnell, M. and Gupta, V. K.: A proof of the Horton law of stream numbers for the Tokunaga model of river networks, Fractals, 16, 227-233, https://doi.org/10.1142/S0218348X08003958, 2008.

Mileyko, Y., Edelsbrunner, H., Price, C. A., and Weitz, J. S.: Hierarchical ordering of reticular networks, PloS one, 7, e36715, https://doi.org/10.1371/journal.pone.0036715, 2012.

Montgomery, D. R. and Dietrich, W. E.: Channel initiation and the problem of landscape scale, Science, 255, 826-830, https://doi.org/10.1126/science.255.5046.826, 1992.

O'Callaghan, J. F. and Mark, D. M.: The extraction of drainage networks from digital elevation data, Computer vision, graphics, and image processing, 28, 323-344, https://doi.org/10.1016/S0734-189X(84)80011-0, 1984.

Ortega, L. and Rueda, A.: Parallel drainage network computation on CUDA, Computers & Geosciences, 36, 171-178, https://doi.org/10.1016/j.cageo.2009.07.005, 2010.

Passalacqua, P., Belmont, P., Staley, D. M., Simley, J. D., Arrowsmith, J. R., Bode, C. A., Crosby, C., DeLong, S. B., Glenn, N. F., and Kelly, S. A.: Analyzing high resolution topography for advancing the understanding of mass and energy transfer through landscapes: A review, Earth-Science Reviews, 148, 174-193, https://doi.org/10.1016/j.earscirev.2015.05.012, 2015.

Peckham, S. D.: Self-similarity in the three-dimensional geometry and dynamics of large river basins, University of Colorado at Boulder1995a.

Peckham, S. D.: New results for self-similar trees with applications to river networks, Water Resour. Res., 31, 1023-1029, https://doi.org/10.1029/94WR03155, 1995b.

https://doi.org/10.5194/egusphere-2026-1128
Preprint. Discussion started: 6 March 2026


Peckham, S. D. and Gupta, V. K.: A reformulation of Horton's laws for large river networks in terms of statistical self-similarity, Water Resour. Res., 35, 2763-2777, https://doi.org/10.1029/1999WR900154, 1999.
Pelletier, J. D.: A robust, two-parameter method for the extraction of drainage networks from high-resolution digital elevation models (DEMs): Evaluation using synthetic and real-world DEMs, Water Resour. Res., 49, 75-89, https://doi.org/10.1029/2012WR012452, 2013.
Perron, J. T., Richardson, P. W., Ferrier, K. L., and Lapotre, M.: The root of branching river networks, Nature, 492, 100-103, https://doi.org/10.1038/nature11672, 2012.
Rinaldo, A., Rigon, R., Banavar, J. R., Maritan, A., and Rodriguez-Iturbe, I.: Evolution and selection of river networks: Statics, dynamics, and complexity, Proceedings of the National Academy of Sciences, 111, 2417-2424, https://doi.org/10.1073/pnas.1322700111, 2014.
Rodriguez-Iturbe, I. and Rinaldo, A.: Fractal river basins: chance and self-organization, Cambridge University Press1997.
Różycka, M. and Migoń, P.: Morphometric properties of river basins as indicators of relative tectonic activity – Problems of data handling and interpretation, Geomorphology, 389, 107807, https://doi.org/10.1016/j.geomorph.2021.107807, 2021.
Salazar, J. F., Villegas, J. C., Rendón, A. M., Rodríguez, E., Hoyos, I., Mercado-Bettín, D., and Poveda, G.: Scaling properties reveal regulation of river flows in the Amazon through a “forest reservoir”, Hydrology and Earth System Sciences, 22, 1735-1748, https://doi.org/10.5194/hess-22-1735-2018, 2018.
Sangireddy, H., Carothers, R. A., Stark, C. P., and Passalacqua, P.: Controls of climate, topography, vegetation, and lithology on drainage density extracted from high resolution topography data, Journal of Hydrology, 537, 271-282, https://doi.org/10.1016/j.jhydrol.2016.02.051, 2016a.
Sangireddy, H., Stark, C. P., Kladzyk, A., and Passalacqua, P.: GeoNet: An open source software for the automatic and objective extraction of channel heads, channel network, and channel morphology from high resolution topography data, Environmental Modelling & Software, 83, 58-73, https://doi.org/10.1016/j.envsoft.2016.04.026, 2016b.
Sassolas-Serrayet, T., Cattin, R., and Ferry, M.: The shape of watersheds, Nature communications, 9, 3791, https://doi.org/10.1038/s41467-018-06210-4, 2018.
Schmitt, R. J., Bizzi, S., Castelletti, A., and Kondolf, G.: Improved trade-offs of hydropower and sand connectivity by strategic dam planning in the Mekong, Nature Sustainability, 1, 96-104, https://doi.org/10.1038/s41893-018-0022-3, 2018.
Schumm, S. A.: Evolution of drainage systems and slopes in badlands at Perth Amboy, New Jersey, Geological society of America bulletin, 67, 597-646, https://doi.org/10.1130/0016-7606(1956)67[597:EODSAS]2.0.CO;2, 1956.
Seybold, H., Rothman, D. H., and Kirchner, J. W.: Climate's watermark in the geometry of stream networks, Geophysical Research Letters, 44, 2272-2280, https://doi.org/10.1002/2016GL072089, 2017.
Shreve, R. L.: Statistical law of stream numbers, The Journal of Geology, 74, 17-37, https://doi.org/10.1086/627137, 1966.
Smart, J. S.: A comment on Horton's law of stream numbers, Water Resour. Res., 3, 773-776, https://doi.org/10.1029/WR003i003p00773, 1967.
Smart, J. S.: Channel networks, in: Advances in hydroscience, Elsevier, 305-346, https://doi.org/10.1016/B978-0-12-021808-0.50011-5, 1972.
Strahler, A. N.: Hypsometric (area-altitude) analysis of erosional topography, Geological society of America bulletin, 63, 1117-1142, https://doi.org/10.1130/0016-7606(1952)63[1117:HAAOET]2.0.CO;2, 1952.
Strahler, A. N.: Quantitative analysis of watershed geomorphology, Eos, Transactions American Geophysical Union, 38, 913-920, https://doi.org/10.1029/TR038i006p00913, 1957.
Tarboton, D. G.: Fractal river networks, Horton's laws and Tokunaga cyclicity, Journal of hydrology, 187, 105-117, https://doi.org/10.1016/S0022-1694(96)03089-2, 1996.
Tejedor, A., Longjas, A., Edmonds, D. A., Zaliapin, I., Georgiou, T. T., Rinaldo, A., and Foufoula-Georgiou, E.: Entropy and optimality in river deltas, Proceedings of the National Academy of Sciences, 114, 11651-11656, https://doi.org/10.1073/pnas.1708404114, 2017.
Thober, S., Cuntz, M., Kelbling, M., Kumar, R., Mai, J., and Samaniego, L.: The multiscale routing model mRM v1.0: simple river routing at resolutions from 1 to 50 km, Geoscientific Model Development, 12, 2501-2521, https://doi.org/10.5194/gmd-12-2501-2019, 2019.
Thorp, J. H., Thoms, M. C., and Delong, M. D.: The riverine ecosystem synthesis: biocomplexity in river networks across space and time, River Research and Applications, 22, 123-147, https://doi.org/10.1002/rra.901, 2006.

https://doi.org/10.5194/egusphere-2026-1128
Preprint. Discussion started: 6 March 2026


Tokunaga, E.: Consideration on the composition of drainage networks and their evolution, Geographical Reports of Tokyo Metropolitan University, 1-27, 1978.

Veitzer, S. A. and Gupta, V. K.: Random self-similar river networks and derivations of generalized Horton laws in terms of statistical simple scaling, Water Resour. Res., 36, 1033-1048, https://doi.org/10.1029/1999WR900327, 2000.

Wang, S. X. and Waymire, E. C.: A large deviation rate and central limit theorem for Horton ratios, SIAM Journal on Discrete Mathematics, 4, 575-588, https://doi.org/10.1137/0404050, 1991.

Ward, J., Tockner, K., Arscott, D. B., and Claret, C.: Riverine landscape diversity, Freshwater biology, 47, 517-539, https://doi.org/10.1046/j.1365-2427.2002.00893.x, 2002.

Whittaker, A. C.: How do landscapes record tectonics and climate?, Lithosphere, 4, 160-164, https://doi.org/10.1130/rf.l003.1, 2012.

Yang, P., Ames, D. P., Fonseca, A., Anderson, D., Shrestha, R., Glenn, N. F., and Cao, Y.: What is the effect of LiDAR-derived DEM resolution on large-scale watershed model results?, Environmental modelling & software, 58, 48-57, https://doi.org/10.1016/j.envsoft.2014.04.005, 2014.

Zanardo, S., Zaliapin, I., and Foufoula-Georgiou, E.: Are American rivers Tokunaga self-similar? New results on fluvial network topology and its climatic dependence, Journal of Geophysical Research: Earth Surface, 118, 166-183, https://doi.org/10.1029/2012JF002392, 2013.

Zhang, L., Dai, B., Wang, G., Li, T., and Wang, H.: The quantization of river network morphology based on the Tokunaga network, Science in China Series D: Earth Sciences, 52, 1724-1731, https://doi.org/10.1007/s11430-009-0176-y, 2009.

Zhang, W. and Montgomery, D. R.: Digital elevation model grid size, landscape representation, and hydrologic simulations, Water Resour. Res., 30, 1019-1028, https://doi.org/10.1029/93WR03553, 1994.